

Central European Journal of Chemistry

Synthesis, characterization and adsorption properties of nanostructured hybrid materials modified by boron and zirconium

Research Article

Ralitsa H. Georgieva¹, Paunka S. Vassileva¹, Albena K. Detcheva^{1*}, Dimitrinka K. Voykova¹, Tsvetelina I. Gerganova², Yordanka Y. Ivanova²

¹Institute of General and Inorganic Chemistry, Bulgarian Academy of Sciences, 1113 Sofia, Bulgaria

²Department of Silicates, University of Chemical Technology and Metallurgy, 1756 Sofia, Bulgaria

Received 7 December 2011; Accepted 13 April 2012

Abstract: The adsorption properties of two new nanostructured hybrid materials containing B₂O₃ and ZrO₂ were studied. The new organic-inorganic materials were synthesized *via* a sol-gel method. As a modifying agent, a quantity of 10 wt.% Zr(OPr)₄ or B(OCH₃)₃ was added. The structure of the hybrid materials was investigated by means of (Fourier transform infrared spectroscopy (FTIR), x-ray diffractometry (XRD), scanning electron microscopy (SEM), (atomic force microscopy (AFM) and nuclear magnetic resonance spectroscopy (NMR). Based on the obtained data, the most probable cross-linking mechanism for the derived gels was proposed. The characterization of texture parameters of both materials was carried out with the use of low-temperature adsorption of nitrogen. Adsorption of Cu(II), Fe(III), Cd(II) and Pb(II) ions on both materials was investigated using multi-component solutions with different concentrations and acidity by means of the batch method. Kinetics of adsorption was also investigated. Pseudo-first order, pseudo-second order and intraparticle diffusion models were used to analyze kinetic data. The adsorption was significantly affected by the pH value. Equilibrium data were fitted to linear Langmuir, Freundlich and Dubinin-Radushkevich models and maximum adsorption capacities were calculated.

Keywords: Nanostructured hybrid materials • Characterization • Adsorption of metal ions • Kinetics • Adsorption equilibrium © Versita Sp. z o.o.

1. Introduction

In the field of materials science the investigations of the relationship between the structure of materials and their properties are of great interest. Sol-gel chemistry offers a unique opportunity for the design of new advance materials with desired properties [1]. The final hybrid materials have the potential for providing interesting combinations of properties which cannot be achieved for other materials [2]. The materials prepared with sol-gel chemistry have been applied to different research fields. It has been established that they are excellent matrices for immobilization of inorganic and organic compounds and various types of biomolecules, including enzymes, whole living cells, antibodies, immune molecules, phospholipids and other proteins [3,4]. Modified silica-

containing materials can be used for technological applications, such as extracting metal ions from aqueous and non-aqueous solutions. These materials show great adsorption capacity and specificity for metal ions [5-8].

The most interesting and promising reagents are the organometallic compounds based on alkoxides of silicon, titanium, aluminium, zirconium and other. This class of potential precursors is very suitable for the solgel technology and is characterized by the presence of –M-O-R (metal-organic bonds) in a metal-network. Selection of molecular or polymeric species of different natures and properties that could also be incorporated into these organic-inorganic systems offers a great number of opportunities [9-14]. In combination with the traditional cross-linking agents such as tetraethylor tetramethylortosilicate, the urea or urethane

groups can be obtained by means of hydrolysis and condensation reactions [9]. Using these reactions, with the participation of trimethylsilyl isocyanate in the solgel synthesis, two possible networks can be obtained – urethanesil or ureasil, depending on the synthesis conditions used [15-19].

Usually, hybrid materials possess a good elasticity, flexibility and higher chemical stability [20] and the gels containing nitrogen and carbon can be used in the field of electronics and optoelectronics [21]. It was proved that the modifying of the siloxane oxicarbonitride network by ZrO2 results in thermally stabile materials [22].

On the other hand, sol-gel borosilicate materials have been systematically studied because of their high temperature resistance. This important property makes them applicable in semiconductor industry, solar thermal technology, optical engineering and in immobilization and disposal of radioactive wastes [23].

Another specific application of both, boron- and zirconium-containing hybride materials is selective layers for gas-separation membranes [24].

In the present work, two novel di-urethanesil hybrid materials modified by boron and zirconium were synthesized and their structure was discussed. The adsorption properties towards Cu(II), Fe(III), Cr(III), Cd(II) and Pb(II) ions for both materials are investigated using multi-component solutions by means of the batch method.

2. Experimental procedure

2.1. Synthesis and characterization of the hybrid materials

The novel di-urethanesil hybrid materials have been prepared as follows: 80 wt.% tetramethoxysilane (TMOS) was dissolved in tetrahidrofurane (THF) in ratio 1:1 and hydrolyzed with acidified water (pH=1.5) for 10 min. After that, 20 wt.% of trimethylsilil isocyanate (TMSI), previously dissolved in THF (1:1) was added. After 30 min of stirring at room temperature, 10 wt.% of zirconium propoxides Zr(OPr)₄ or 10 wt.% of trimethyl borate B(OCH₃)₃ as modifying agents in the presence of ethylacetoacetate (EtAcAc) in ratio 1:1 or izopropanol (PrOH) in ratio 1:3, respectively, were added [15,16,25]. The mixtures were further stirred for 40 min. After drying at 60°C, monolith solid materials were obtained. For the adsorption experiments, pieces of these materials were used after grinding them in agate mortar.

The schematic diagram for the preparation of the hybrid materials containing B and Zr is shown in Fig. 1.

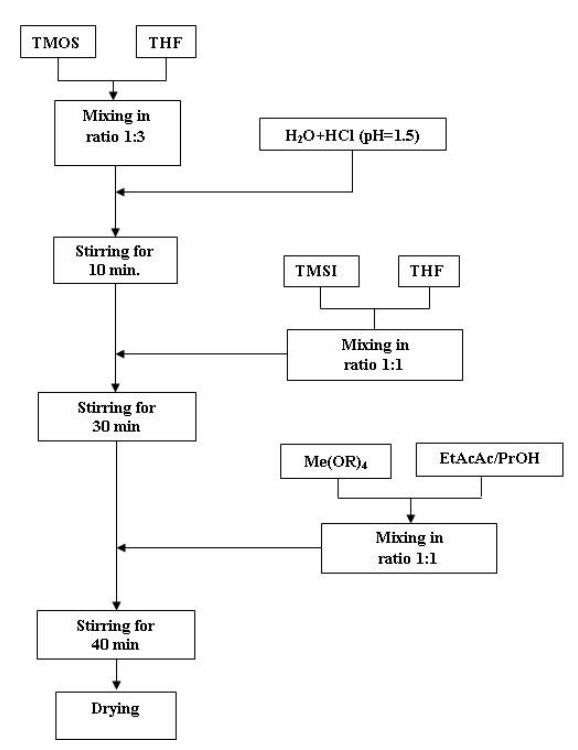


Figure 1. Schematic diagram for the synthesis of the hybrids materials containing Zr and B.

The structure of the derived xerogels denoted as Si-10B or Si-10Zr was investigated by means of XRD on a X-Ray Diffractometer System "Geigetflex" D/Max- C Series (Rigaκu, Japan) by 30 mA, 40 V, with Cu-Kα radiation; FTIR (Mattson 7000, USA) in the range of 4000-400 cm⁻¹ in KBr-pellets and SEM (S4000 Field Emission, Hitachi, Japan). Atomic Force Microscope measurements were performed on AFM NanoScope IIIA Tapping ModeTM, (USA). Nuclear Magnetic Resonance NMR spectra for solid state ²⁹Si were recorded at 79.79 MHz on a Bruker Avance 400 spectrometer (Germany).

The characterization of texture parameters of both materials was carried out by low-temperature adsorption (at 77 K) of nitrogen using Gemini model 2370V5.00, Micrometrics, (UK). The nitrogen adsorption isotherms were analyzed to evaluate the following parameters: the specific surface area, the total pore volume and average pore radius.

2.2. Adsorption studies

The adsorption properties of Si-10B and Si-10Zr with respect to Cu(II), Fe(III), Pb(II), Cr(III) and Cd(II) ions in multi-component solutions were determined by means of the batch method. Experiments were carried out using stoppered 50 mL Erlenmeyer flasks containing about 0.1 g Si-10B or Si-10Zr sample and 10 mL of aqueous solution containing all metal ions under study. The

mixture was shaken at room temperature for 5 hours by an automatic shaker. After reaching the equilibrium, the adsorbent was removed by filtration through a Millipore filter (0.2 μ m). The initial and equilibrium concentrations of the metal ions were determined by flame AAS on a Pye Unicam SP 192 flame atomic absorption spectrometer (UK).

The effect of acidity on the removal efficiency of the adsorbents studied was investigated over the pH range 2.0–5.5 (pH-meter model pH 211, Hanna instruments, Germany) and with employing initial concentration of 20 mg L⁻¹ for all investigated ions. This allowed the optimal pH value for each metal ion to be established. At this optimal pH value, adsorption of the metal ions concerned is significant and no precipitation of metal hydroxide occurs. Thus, to determine the effect of the initial metal ion concentration on the adsorption capacity initial concentrations in the range 5–100 mg L⁻¹ at pH 5.0 were chosen.

Analytical grade reagents were used in all experiments. The working solutions containing different concentrations of Cu(II), Fe(III), Pb(II), Cr(III) and Cd(II) ions were prepared by stepwise dilution of the stock solutions (Titrisol Merck, Germany). All adsorption experiments were replicated and the average results were used in data analyses.

3. Results and discussion

3.1. Characterization of the hybrid materials

The structure of Si-10B and Si-10Zr was investigated by means of FTIR, XRD, SEM, AFM and NMR.

3.1.1. FTIR investigations

The FTIR spectra for the synthesized hybrid materials are presented in Fig. 2. There is an indirect evidence that no there was no remaining trimethylsilyl isocyanate after the sol-gel synthesis. This was established based on the lack of band corresponding to the free -NCO- groups at 2300 cm⁻¹. The main signals due to Si-O-Si bonds (1063 cm⁻¹ and 435 cm⁻¹), and Si-(CH₃)₃ bonds are registered at 1254 cm⁻¹ for (CH)₃, at 845 cm⁻¹ for Si–CH₃ and at 765 cm⁻¹ Si–C [26-28]. Additional vibration peaks in the range of 1636 cm⁻¹ and 1750 cm⁻¹ appeared due to the urethane group (NH-CO-O) vibrations [29]. For the xerogel modified by 10 wt.% trimethyl borate, peaks in the region of 1500 cm^{-1} – 1300 cm^{-1} due to (v B–O) are also present. The bands due to adsorbed water (at 3300 cm⁻¹) are present in both spectra and the intensity of the signal is sharper in the gel modified by boron. This suggests the surface area escalation of Si10B and the increasing levels of M–OH (M=B, Si) terminal groups. For Si-10Zr, an increased intensity of the Si–OH stretching vibration was observed at 950 cm⁻¹. Moreover, from the FTIR patterns obtained, it was established that in both hybrid gels the organic and inorganic building blocks were linked to each other by covalent bonds (Si–NH₂ and Si–(CH₃)₃) forming single homogeneous nanostructured material [30].

The band at 1400 cm⁻¹ in the spectrum of Si-10B can be attributed to B-OH free groups and it suggests the presence of additional acceptor centers on the surface of this material. Thus, we expect enhanced adsorption activity for Si-10B as compared with Si-10Zr.

3.1.2. XRD-analysis

Fig. 3 shows the XRD patterns of the derived xerogels Si-10B and Si-10Zr. Both materials are amorphous. For Si-10B in the range between 10 and 35° 29 crystal phase due to B(OH)₃ was also registered.

3.1.3. SEM-analysis

The morphology of the hybrids modified by 10 wt.% B and Zr have been investigated by SEM (Figs. 4a and 4b). It is visible that the gel modified by boron, Fig. 4a, exhibits in the most degree open porosity with its characteristic pore size detected to be between 0.5 μ m and 1 μ m. The presence of pores in this formulation is due to the rapid hydrolysis and condensation process followed by grain growth of boron hydroxide in the wet gel material. After gel curing at 60°C, partial decomposition of boron hydroxide appeared and regularly distributed asymmetrical pores were formed [31].

According to the IUPAC nomenclature, the described hybrid gel can be related to the macro-porous class of materials.

For comparison, SEM image of gel modified by zirconium is presented is Fig. 4b. At the same microscale level, no pores, crystals, and cracks are observed. This can be related to the influence of the modifying ions used in the materials' preparation. It is possible, that at precursor concentration of 10%, zirconium is acting more as cross-linking agent, rather than modifier of the silica backbone.

3.1.4. AFM-analysis

In order to determine the Root Mean Square (RMS) surface roughness, the topography of samples has been studied by means of AFM. The fresh fractured surfaces were prepared by breaking the monolithic samples immediately prior to the measurements. In general, the topographic features obtained with AFM were found to depend on the modifying ions in gel

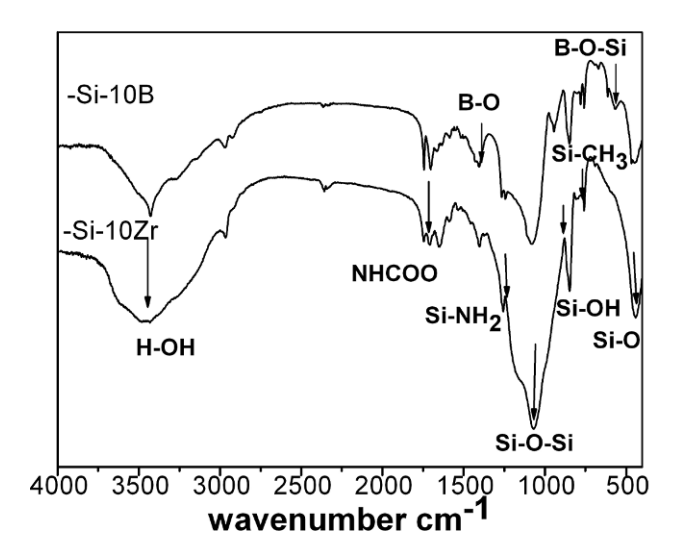


Figure 2. IR spectra of nanostructured hybrid materials Si-10B and Si-10Zr.

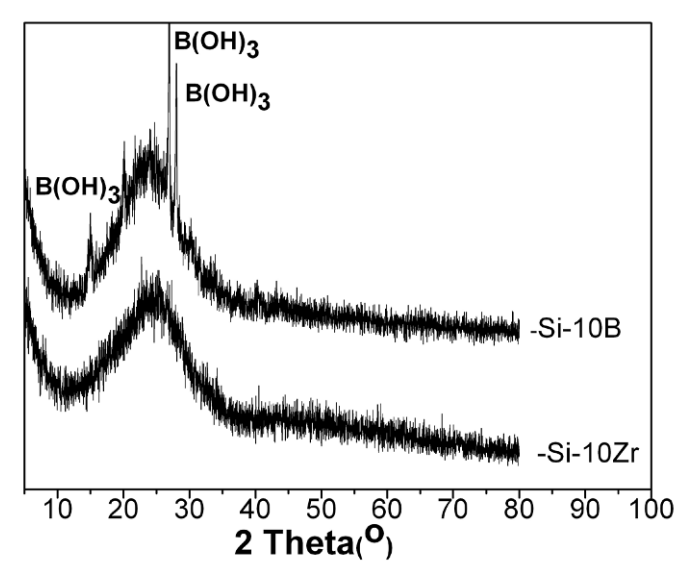


Figure 3. XRD patterns of nanostructured hybrid materials Si-10B and Si-10Zr.

networks. The results from this study are presented on Fig. 5 as 3D images.

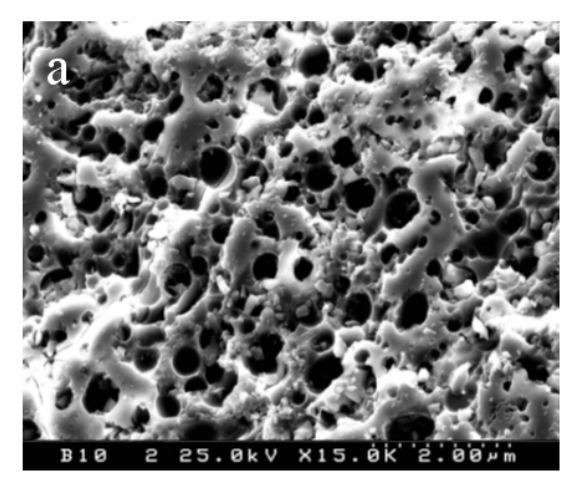
The sample Si-10Zr (Fig. 5b) exhibits a smooth and relatively featureless surface. In sharp contrast, the Si-10B sample (Fig. 5a) shows clearly discernible pore domains in the range of 0.5 μ m to 1 μ m. The morphological characteristics are also reflected in the surface roughness values. The average RMS roughness for Si-10Zr gel was detected to be 0.6 nm in comparison with RMS of Si-10B sample, where its value was much larger (1.3 μ m).

AFM results are in a good agreement with SEM micrographs and they show that the morphology of the gel material depends on the modifying ion in the material's network.

3.1.5. NMR-analysis

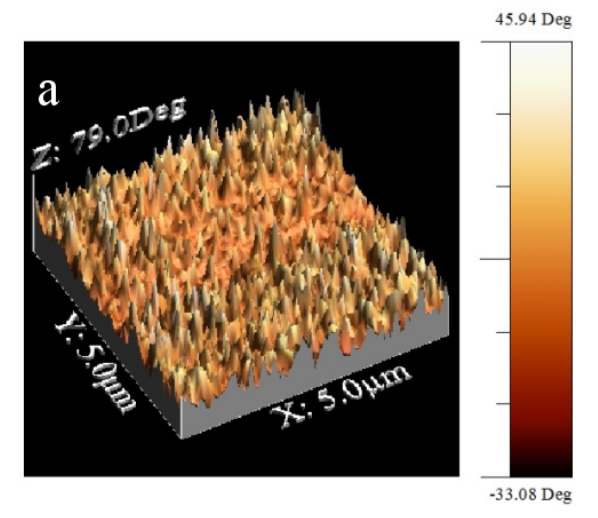
The variation of ²⁹Si CP MAS NMR spectra of the hybrid materials with different modifying ions has been studied (Fig. 6). The obtained NMR spectra are characterized by signals at –91, –101 and –111 ppm attributed to different Si units namely Q2 [Si(OSi)₂(OCH3)₂], Q3 [Si(OSi)₃OCH₃] and Q4 [Si(OSi)₄], respectively [32]. The presence of Q2 structural units suggests that the condensation process is initiated and makes the sample very active at atmosphere conditions.

Moreover, a signal at +14 ppm is observed in the two NMR spectra. From the bibliographic data, this signal is due to M [(CH)₃SiN] structural units [33], which allow to conclude that during the hydrolysis –condensation reactions, the Si–N and Si–C bonds, typical of TMSI



b 22r10 25.0kV X15.0k 2:00 jim

Figure 4. SEM micrographs of a) Si-10B and b) Si-10Zr.



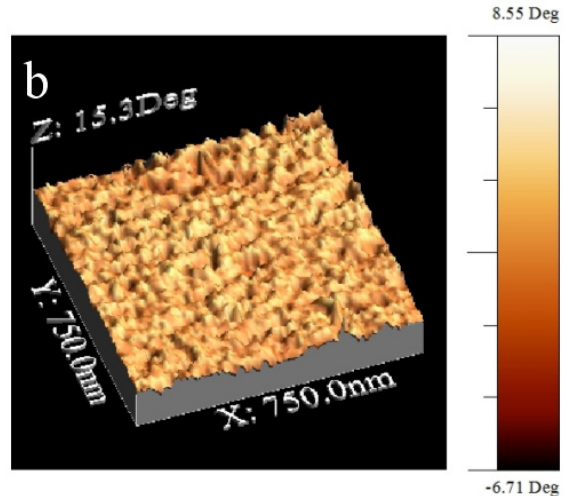


Figure 5. AFM images of a) Si-10B and b) Si-10Zr.

as a precursor, remain stable. When Zr, instead of B is used in the synthesis of the hybrid urethanesiles, a decrease in the intensity of Q4 (all four oxygen atoms of the ${\rm SiO}_4$ -tetrahedra linked to other polyhedra) structural units is observed at the expense of Q3 units (three oxygen linkages to silicon, one OH group). This is due to the formation of Zr-O-Si bonds in the gel network. For boron-modified urethanesiles, the gel structure is formed by ${\rm BO}_3$ and ${\rm BO}_4$ units [25].

3.1.6. BET-analysis

The low temperature nitrogen adsorption on the derived xerogels Si-10B and Si-10Zr is expressed by I-type isotherm (Fig. 7). The nitrogen adsorption isotherms were used for evaluation of textural parameters and following values were obtained as follows:

- Si-10B - specific surface area - 630 m^2 $g^{\text{-1}};$ total pore volume - 0.51 cm^3 $g^{\text{-1}}$ and average pore radius

- 1.6 nm.
- Si-10Zr specific surface area 520 m^2 $g^{\text{-1}};$ total pore volume 0.44 cm^3 $g^{\text{-1}}$ and average pore radius 1.7 nm.

3.2. Adsorption studies

Most industrial wastewaters contain different metal ions and the presence of co-cations can affect their sorption [34]. In the present paper competitive sorption of Pb(II), Cu(II), Cr(III), Fe(III) and Cd(II) onto Si-10B and Si-10Zr in multi-component aqueous solutions was investigated. Metal sorption efficiency of the adsorbents as a function of concentration and pH at different contact times was studied.

3.2.1. Kinetic studies

Fig. 8 shows the effect of contact time for the sorption of Pb(II), Cu(II), Cr(III), Fe(III) and Cd(II) onto Si-10B and Si-10Zr. It is evident that the sorption capacity increases

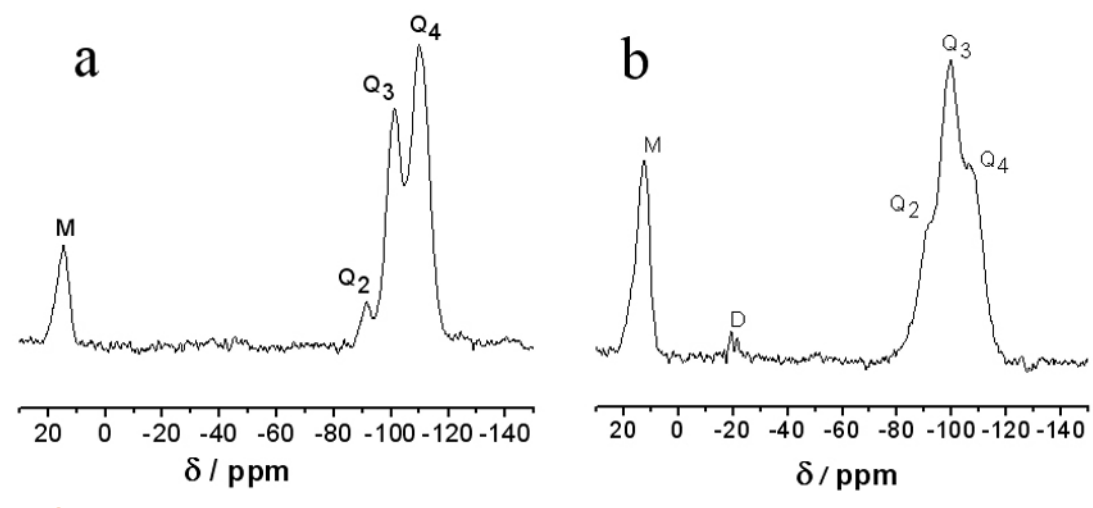


Figure 6. 29Si NMR spectra of a) Si-10B and b) Si-10Zr.

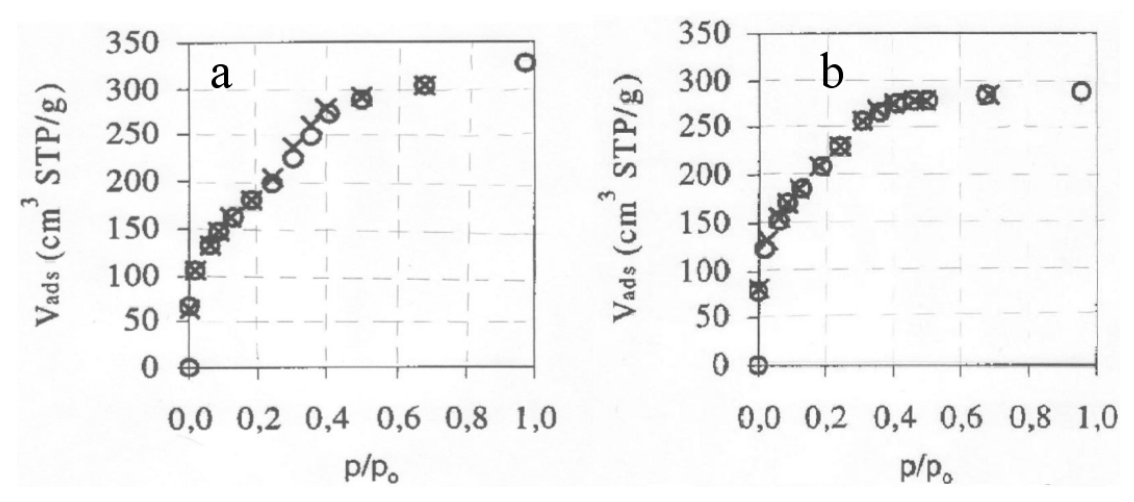


Figure 7. Low temperature nitrogen adsorption isotherm on a)Si-10B and b)Si-10Zr.

with increase in contact time. It is found that equilibrium is attained at two hours.

The mechanism of the adsorption of multi-component aqueous solutions was tested using the pseudo-first-order, the pseudo-second-order and the intraparticle diffusion model.

The linear form of pseudo first-order equation is given by [35]:

$$log (Qe - Qt) = log (Qe) - (k/2.303)t$$
 (1)

where $\mathbf{Q}_{\mathbf{e}}$ and $\mathbf{Q}_{\mathbf{t}}$ are the amounts of Pb(II), Cu(II), Cr(III), Fe(III) and Cd(II) adsorbed at equilibrium and certain time (t) respectively, $\mathbf{k}_{\mathbf{1}}$ is the rate constant. Plots of log (QeQt) *versus* t are linear and the adsorption rate constants $\mathbf{k}_{\mathbf{1}}$ and theoretical \mathbf{Qe} values can be calculated.

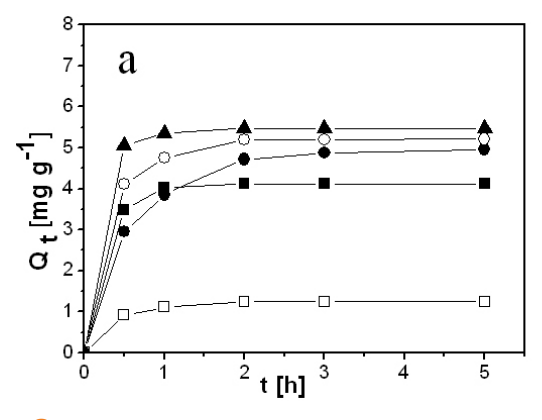
Applicability of the pseudo-second-order kinetics is tested with the following equation [36]:

$$(t/Qt) = (1/k_2Qe) + (1/Qe)t$$
 (2)

where; $\mathbf{k_2}$ is the pseudo-second order rate constant. $\mathbf{k_2}$ and $\mathbf{Q_e}$ values were determined from the slope and intercept of $\mathbf{Q_t}$ versus t plots.

The values of the parameters and correlation coefficients for both models are presented in Table 1. The results show that the fit with the pseudo-second order adsorption model is very good (correlation coefficients $r^2 \geq 0.998$) and the calculated equilibrium adsorption capacities, $\mathbf{Q}_{\mathbf{e}}$ are close to experimental data. Therefore we assume that the pseudo-second order adsorption mechanism is predominant for all investigated ions, suggesting that the rate-limiting step is the chemical adsorption.

In order to assess the nature of the diffusion process responsible for the adsorption of the investigated ions onto the hybrid material, attempts were made to



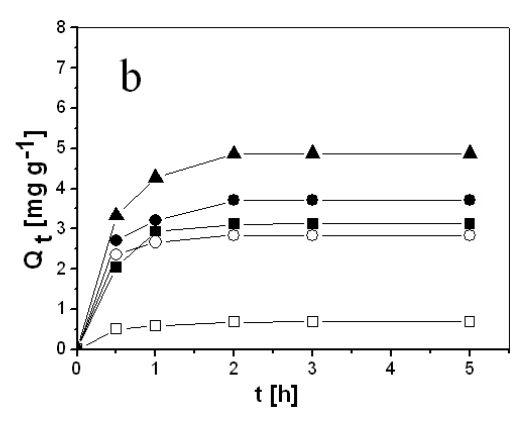


Figure 8. Effect of contact time on the amount of adsorbed Fe(III)- ■, Cr(III)- ●, Cd(II)- □, Cu(II)- ○ and Pb(II)- ▲ ions (C₀ 10 mg L¹ pH 5.00) on a)Si-10B and b)Si-10Zr.

calculate the pore diffusion coefficients. The intraparticle diffusion equation [37,38] is expressed as:

$$Qt = k_{id} t^{1/2} + C (3)$$

where ${\bf C}$ is the intercept, and ${\bf k}_{\rm id}$ is the intraparticle diffusion rate constant (mg g-1 min1/2). According to this model, the plots Qt versus t1/2 should be linear if the intraparticle diffusion is involved in the adsorption process and if these lines pass through the origin. In such case, the intraparticle diffusion is the ratecontrolling step [39]. When the plots do not pass through the origin, this indicates some degree of boundary layer control and shows that the intraparticle diffusion is not the only rate-limiting step, but also that the other kinetic models may control the rate of adsorption, all of which may be operating simultaneously. The slopes of linear portion from the figure can be used to derive values of the rate parameter, $\mathbf{k}_{\mathrm{id}},$ for the intraparticle diffusion. Values of the intercept C give an idea about boundary layer thickness, where the larger intercept indicates a greater boundary layer [40,41]. The values of \mathbf{k}_{id} and C are presented in Table 1. The deviation of straight lines from the origin indicates that intraparticle diffusion cannot be accepted as the only rate-determining step for the adsorption of investigated ions on Si-10B and Si-10Zr. The correlation coefficients for the intraparticle diffusion model are also lower than those for the pseudo-second-order kinetic model. These results confirm that the pseudo-second-order mechanism is predominant in the adsorption of Cu(II), Fe(III), Cr(III), Cd(II) and Pb(II) onto Si-10B and Si-10Zr.

In case of all investigated ions, the calculated values of \mathbf{k}_{id} for Si-10B are higher than those obtained for Si-10Zr. This result indicates that Si-10B is more porous than Si-10Zr [42], which is supported by results from SEM, AFT and BET-analysis discussed above.

3.2.2. Effect of pH on adsorption efficiency

Since the binding of metal ions by surface functional groups was strongly pH dependent, the pH of the aqueous solution is an important controlling parameter in the adsorption process.

The influence of pH on the amounts of adsorbed metal ions on both hybrid materials was studied in the pH range from 2.0 to 5.5 (Fig. 9). The pH was limited to values equal to 5.5 because of precipitation of metal hydroxide at higher pH values. As expected, the adsorption of the investigated metal ions strongly depends on acidity of the initial solutions. With the increase of pH-values the amounts of adsorbed ions increases and the optimum pH range is found to be above 5.0. Similar observations have been reported for adsorption of metal ions on different adsorbents [34,43-47]. Most affected by pH changes is the adsorption of Pb(II).

3.2.3. Adsorption isotherms

The effects of metal ions' concentrations on their adsorption are shown on Fig. 10. Both hybrid materials show highest affinity towards Pb(II) ions, and lowest – for Cd(II) ions.

The adsorption isotherms described the adsorption equilibrium of the investigated ions at constant temperature. The different models are used to estimate the adsorption equilibrium data. Thus, the experimental data obtained were fitted to Langmuir, Freundlich and Dubinin–Radushkevich isotherm equations to determine the most suitable sorption mechanism.

Langmuir isotherm

The linear form of the Langmuir isotherm is expressed by the following equation:

$$C_{o}/Q_{o} = 1/K_{o}Q_{o} + C_{o}/Q_{o} \tag{4}$$

Table 1. Kinetic parameters of adsorption of Fe(III), Cr(III), Cd(II), Cu(II) and Pb(II) ions from aqueous solutions onto Si-10B and Si-10Zr.

Adsorbents	Metal ions	Pseudo-first order constants			Pseudo-second order constants			Intrapartic cons			
		Q _e (mg g ⁻¹)	K ₁ (min ⁻¹)	r²	Q _e (mg g ⁻¹)	K ₂ (min ⁻¹)	r²	k _{id} (mg g ⁻¹ min ^{-1/2})	C (mg g ⁻¹)	r²	Q _{e, exp} (mg g ⁻¹)
	Fe(III)	2.91	0.056	0.995	4.18	0.282	0.999	1.682	1.35	0.785	4.12
Si-10B	Cr(III)	3.89	0.053	0.999	5.35	0.045	0.999	2.179	0.98	0.907	4.97
	Cd(II)	2.26	0.021	0.977	1.30	0.103	0.998	0.533	0.33	0.845	1.25
	Cu(II)	2.39	0.058	0.966	5.35	0.140	0.999	2.176	1.52	0.822	5.21
	Pb(II)	3.40	0.062	0.986	5.51	0.531	0.999	2.181	1.94	0.756	5.52
	Fe(III)	4.62	0.051	0.998	3.26	0.093	0.998	0.136	0.79	0.848	3.12
Si-10Zr	Cr(III)	5.16	0.045	0.972	3.87	0.065	0.999	1.587	0.97	0.852	3.73
	Cd(II)	0.56	0.033	0.978	0.72	0.030	0.999	0.293	0.18	0.849	0.69
	Cu(II)	2.28	0.038	0.994	2.89	0.204	0.999	1.167	0.89	0.800	2.83
	Pb(II)	7.06	0.066	0.968	5.09	0.285	0.999	2.106	1.21	0.859	4.89

where \mathbf{C}_{e} is the concentration of metal ions in the equilibrium solution (mg L⁻¹), \mathbf{Q}_{e} is the amount of ion adsorbed (mg) per unit mass of adsorbent (g), \mathbf{Q}_{o} , the maximum adsorption capacity (mg g⁻¹); \mathbf{K}_{L} is the Langmuir constant related to enthalpy of the process.

The essential characteristics of Langmuir isotherm can be expressed in terms of a dimensionless constant or separation factor, R_i , which is defined as:

$$R_{L} = 1/\left(1 + K_{L}C_{o}\right) \tag{5}$$

The \mathbf{Q}_o and \mathbf{K}_L values obtained from these plots are listed in Table 2. The \mathbf{Q}_o values for Si-10B vary from 4.37 mg g⁻¹ for cadmium ions to 12.15 mg g⁻¹ for lead ions and for Si-10Zr from 3.83 mg g⁻¹ for cadmium ions to 10.99 mg g⁻¹ for lead ions. It is obvious that highest equilibrium adsorption capacity \mathbf{Q}_o was obtained for the Pb(II) ions.

The Langmuir model supports the following hypothesis: the adsorbent has a uniform surface: absence of interactions between the solid molecules; the sorption process takes place in a single layer. According the correlation coefficients r^2 (Table 2) the fit to this model is very good.

The Langmuir parameters can be used to predict the affinity between the adsorbate and adsorbent using the dimensionless separation factor R_L . The R_L values for the investigated adsorbent are found to vary within the ranges: 0.025 - 0.826 (for Si-10B) and 0.052 – 0.906 (for Si-10Zr). All values are between 0 and 1 which indicates a favourable adsorption for all investigated ions. In addition, the values of the separation factor

 (R_L) prove that the nanostructured hybrid materials Si-10B and Si-10Zr are potential adsorbents for Pb(II), Cu(II), Fe(III), Cd(II) and Cr(III) removal from aqueous solutions.

Freundlich isotherm

The linear form of the Freundlich model is expressed by the following equation:

$$ln Q_e = lnk_F + (1/n) lnC_e$$
 (6)

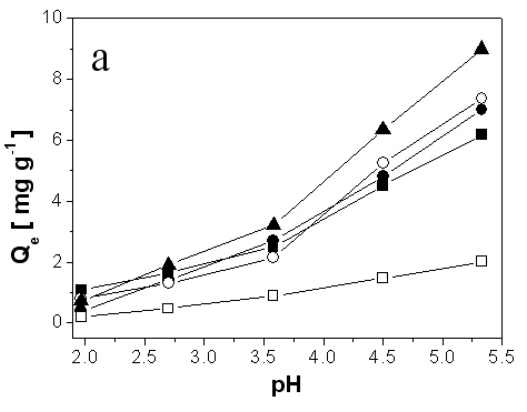
where k_F is a constant related to the adsorption capacity and n is an empirical parameter related to the intensity of adsorption.

The empirical Freundlich isotherm is based on the assumption that the adsorption sites are distributed exponentially with respect to the heat of adsorption. The values of kF and n were calculated from the intercepts and slopes of the linear Freundlich plots respectively and are shown on Table 2.

On the basis of the correlation coefficients (r2) there is a good agreement between the Freundlich model and our experimental data but not as good as for the Langmuir model. All n- values are greater than 1 (Table 2), indicating that both materials exhibit good adsorption properties over the entire range of metal concentrations studied.

Dubinin-Radushkevich isotherm

The Dubinin–Radushkevich (D-R) isotherm reveals the adsorption mechanism based on the potential theory. The linear form of the D–R isotherm is described by the



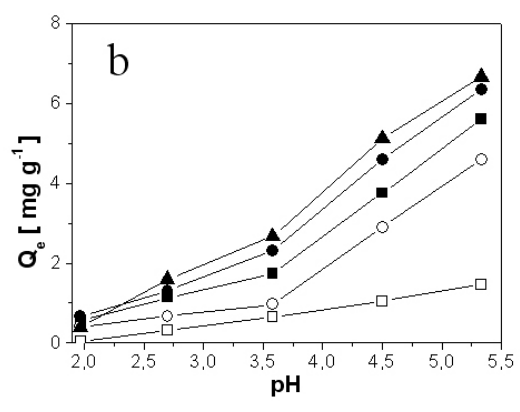
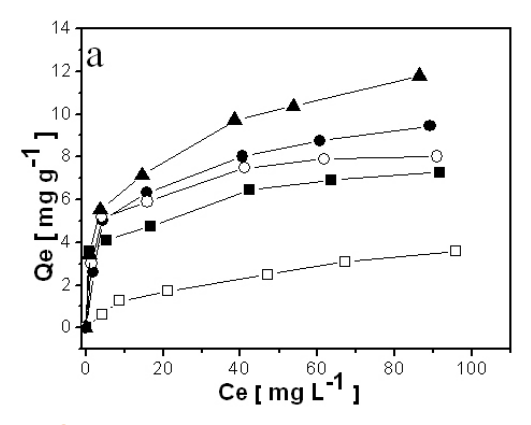


Figure 9. The effect of pH on metal adsorption of Fe(III)- ■, Cr(III)- □, Cu(II)- □, Cu(II)- ○ and Pb(II)- ▲ ions on a) Si-10B and b)Si-10Zr.



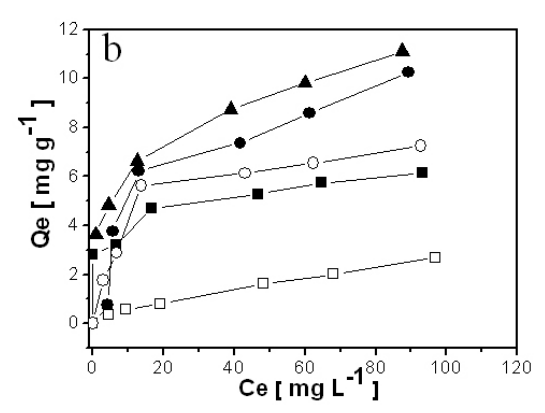


Figure 10. Adsorption isotherms for multi-component solutions of Fe(III)- ■, Cr(III)- ●, Cd(II)- □, Cu(II)- ○ and Pb(II)- ▲ ions on a)Si-10B and b)Si-10Zr.

following equation:

$$\ln Q_{\rm e} = \ln Q_{\rm m} - \beta \varepsilon^2 \tag{7}$$

where \mathbf{Q}_{e} is the amount of metal ion (mg) adsorbed per unit mass of adsorbent (g), \mathbf{Q}_{m} is the maximum adsorption capacity (mg g⁻¹), $\boldsymbol{\beta}$ is the adsorption energy constant (mol² J⁻²), and $\boldsymbol{\varepsilon}$ is the Polanyi potential, described as:

$$\varepsilon = RT \ln(1 + 1/C_{\Delta}) \tag{8}$$

where R is the gas constant (J mol⁻¹K⁻¹) and T is the temperature (K). The mean adsorption energy E (kJ mol⁻¹) can be calculated using the parameter β as follows:

$$E = 1/(-2\beta)^{1/2} \tag{9}$$

According the correlation coefficients r^2 (values from 0.687 to 0.982, Table 2), fit of this model is worse than for the other two models.

The value of E is very useful in predicting the type of adsorption and give information about chemical

and physical adsorption. It is known that energy of adsorption in the range of 2–20 kJ mol⁻¹ could be considered physisorption in nature [49]. Physical means that electrostatic force plays a significant role in adsorption mechanism. As shown in Table 2, the values obtained in the present work are in the range of 5.19 to 9.05 kJ mol⁻¹. This indicates that the type of adsorption for all investigated ions onto both nanostructured hybrids materials is essentially physical.

It is important to assume that the mechanism of metal ions adsorption on the nanostructured hybrids materials containing boron or zirconium cannot be attributed directly to the Langmuir, Freundlich or Dubinin–Radushkevich models. However, from data listed in Table 2, it can be concluded that the adsorption isotherm of the investigated ions exhibits mainly Langmuir behaviour, which indicates homogeneous surface binding. It also confirms the existence of mainly monolayer adsorption.

The adsorption capacities of all investigated ions towards both hybrid materials do not differ substantially. Thus the hybrid materials in the present study could be used for the simultaneous removal

Table 2. Isotherm constants for adsorption of metal ions on Si-10B and Si-10Zr.

Adsorbents	Metal Ions	Langmuir parameters			Freundlich	n paramete	Dubinin-Radushkevich parameters			
		Q ₀ (mg g ⁻¹)	K ₁ (L mg ⁻¹)	r²	k _F (mg ^{1 - n} L ⁿ g ⁻¹)	n (L mg ⁻¹)	r²	Q _m (mg g ⁻¹)	E (KJ mol ⁻¹)	r²
Si-B10	Fe(III)	7.43	0.293	0.997	3.44	6.19	0.959	3.59	9.05	0.980
	Cr(III)	9.90	0.173	0.996	2.55	3.28	0.907	3.24	7.24	0.820
	Cd(II)	4.37	0.042	0.977	0.34	1.93	0.972	1.58	5.89	0.931
	Cu(II)	8.05	0.396	0.999	3.17	4.56	0.899	3.69	8.47	0.766
	Pb(II)	12.15	0.203	0.993	3.61	3.71	0.992	4.24	9.24	0.914
Si-10Zr	Fe(III)	6.37	0.185	0.994	2.51	5.10	0.929	2.91	8.78	0.910
	Cr(III)	10.61	0.030	0.871	1.19	1.83	0.855	2.49	6.06	0.835
	Cd(II)	3.83	0.021	0.891	0.12	1.48	0.994	0.28	5.19	0.982
	Cu(II)	7.08	0.133	0.996	1.43	2.66	0.827	2.26	6.98	0.687
	Pb(II)	10.99	0.184	0.983	3.69	4.89	0.978	4.01	9.29	0.900

of the investigated ions from aqueous solutions. Better adsorption properties were observed by Si-10B which could be explained with its structure and surface properties - additional acceptor centers, higher specific surface area and total pore volume.

4. Conclusions

The adsorption of Cu(II), Fe(III), Cr(III), Cd(II) and Pb(II) from aqueous solutions onto two new nanostructured hybrid materials Si-10B and Si-10Zr was studied. The structure of the hybrid materials was investigated by means of FTIR, XRD, SEM, AFM and NMR. Using the FTIR and 29Si NMR studies, the most probable cross-linking mechanism by formation of both materials was proposed. These analyses proved the presence of covalent bonds between the organic and inorganic parts, which classified Si-10B and Si-10Zr as nanostructured materials. It was proven that both materials were amorphous. The AFM results are in a good agreement with SEM micrographs and show that the morphology of the gel material depends on the type of modifying ion in the material's network.

References

- [1] T.Gunji, M. Okogawa, M. Hongo, Y. Abe, J. Polym. Sci., Part A: Polym. Chem. 43, 763 (2005)
- [2] M.C. Goncalves, V. de Z. Bermudez, D. Ostrovskii,L.D. Carlos, Electrochim. Acta 48, 1977 (2003)
- [3] G. Chernev, B. Borisova, L. Kabaivanova, I.M. Salvado, Cent. Eur. J. Chem. 8, 870 (2010)
- [4] L. Kabaivanova, G. Chernev, I.M. Salvado, M.H.V. Fernandes, Cent. Eur. J. Chem. 9, 232 (2011)

obtained by low-temperature nitrogen adsorption reveals that porous and texture parameters for Si-10B are better when compared with Si-10Zr. The influence of acidity of initial metal ion solutions on their adsorption was investigated and the optimum pH range was found to be about 5.0. The pseudo-second order kinetic model showed best correlation to experimental data. It was shown that Langmuir isotherm most adequately described the adsorption process. In all cases, the highest adsorption capacity was achieved for Pb(II) ions, and the lowest one for Cd(II). Both materials showed good adsorption properties towards Cu(II), Fe(III), Cr(III), Cd(II) and Pb(II) ions and could be used for the simultaneous removal of the investigated ions from aqueous solutions. Better adsorption properties were observed for Si-10B which could be explained with its structure and surface properties - additional acceptor centers, higher specific surface area and total pore volume.

Acknowledgements

The authors kindly acknowledge the financial support by the National Centre for New Materials UNION (Contract No DCVP-02/2/2009).

- [5] P. Tzvetkova, P. Vassileva, N. Nikolova, L. Lakov, O. Peshev, J. Mater. Sci. 39, 2209 (2004)
- [6] M.E. Mahmoud, O.F. Hafez, M.M. Osman, A.A. Yakout, A. Alrefaay, J. Hazard. Mater. 176, 906 (2010)
- [7] A. Detcheva, P. Vassileva, R. Georgieva, D. Voykova, T. Gerganova, Y. Ivanova, Cent. Eur. J. Chem. 9, 932 (2011)
- [8] A. Detcheva, P. Vassileva, R. Georgieva, Compt.

- Rend. Acad. Bulg. Sci. 64, 815 (2011)
- [9] M.M. Silva, S.C. Nunes, P.C. Barbosa, A. Evansa, V. de Z. Bermudez, M.J. Smith, D. Ostrovskii, Electrochim. Acta 52, 1542 (2006)
- [10] S. Dire, R. Ceccato, F. Babonneau, J. Sol-Gel Sci. Technol. 34, 53 (2005)
- [11] A. Al Jaafari, Am. J. App. Sci. 7, 171 (2010)
- [12] C.B. Sih, O.M. Wolf, Chem. Commun. 27, 3375 (2005)
- [13] C. Sanchez, B. Julián, P. Belleville, M. Popall, J. Mater. Chem. 15, 3559 (2005)
- [14] P. Gómez-Romero, K. Cuentas-Gallegos, M. Lira-Cantu, N. Casan-Pastor, J. Mater. Sci. 40, 1423 (2005)
- [15] Y. Ivanova, Y. Dimitriev, T. Gerganova, R. Bryaskova, M.H.V. Fernandes, I.M. Salvado, Cent. Eur. J. Chem. 3, 452 (2005)
- [16] Y. Ivanova, T. Gerganova, Y. Dimitriev, I.M. Salvado, M.H.V. Fernandes, Thin Solid Films. 515, 271 (2006)
- [17] Y. Ivanova, T. Gerganova, Y. Dimitriev, I. Salvado, M. Fernandes, A.Wu, Phys. Chem. Glasses: Eur. J. Glass. Sci. Technol. B48, 251 (2007)
- [18] Y. Ivanova, Ts. Gerganova, M.H.V. Fernandes, I.M. Salvado, Cent. Eur. J. Chem. 7, 42 (2009)
- [19] Y. Ivanova, T. Gerganova, Y. Vueva, I.M.M. Salvado, M.H.V. Fenandes, Inter. J. Nanomanufacturing 5, 152 (2010)
- [20] T.R.R. Saraidarov, A. Saschiuk, E. Lifshitz, J. Sol-Gel Sci. Technol. 26, 533 (2003)
- [21] P. Colombo, J. Sol-Gel Sci. Technol. 2, 601 (1994)
- [22] M. Guglielmi, J. Sol-Gel Sci. Technol. 8, 443 (1997)
- [23] S. Sakka, Handbook of sol-gel science and technology-processing, characterization and applications (Kluwer Academic Publishers, New York, 2004)
- [24] M. Smaihi, J.-C.Schrotter, C. Lesimple, I. Prevost, C. Guizard, J. Memb. Sci. 161, 157 (1999)
- [25] T. Gerganova, Y. Ivanova, I.M.M. Salvado, M.H.V. Fernandes, In: R. Morris (Ed.), The Sol-Gel Process: Uniformity, Polymers and Applications, Chapter 12: Isocyanate modified silanes as a new generation precursors in the sol-gel technology: From materials design to application (Nova Science Publishers, Inc, New York, 2010) 495
- [26] H. Günzler, H. Gremlich, H. Heise, M. Blumich, IR Spectroscopy: An Introduction (Wiley-VCH Verlag GmbH & Co. KGaA, Weinheim, 2002)
- [27] B. Stuart, Infrared Spectroscopy: Fundamentals and Applications, (John Wiley and Sons Ltd, Chichester, UK, 2004)

- [28] B. Smith, Fundamentals of Fourier Transform Infrared Spectroscopy (CRC Press, New York, 1996)
- [29] R. Pena-Alonso, J. Rubio, F. Rubio, J.L. Oteo, J. Sol-Gel Sci. Tech. 25, 255 (2002)
- [30] G.D. Soraru, S.M. Guadagnino, P. Colombo, J. Egan, C. Pontano, J. Am. Ceram. Soc. 85, 1529 (2002)
- [31] A.S. Abd-El-Aziz, C.E. Carraher, C.U. Pittman, M. Zeldin, In: R.H. Neilson (Ed.), Macromolecules Containing Metal and Metal-Like Elements, Volume 8: Boron-Containing Polymers, (John Wiley & Sons, Inc., Hoboken, New York, 2007)
- [32] K.J.D. Mackenzie, M.E. Smith, Multinuclear Solidstate NMR of Inorganic Materials (Elsevier Science Ltd, New York, 2002)
- [33] R. Corriu, Eur. J. Inorg. Chem. 2001, 1109 (2001)
- [34] P. Vassileva, A. Detcheva, Adsorpt. Sci.Technol. 28, 229 (2010)
- [35] H. Leinonen, J. Letho, Waste Manag. Res. 19, 45 (2001)
- [36] Y.S. Ho, G. Mckay, Process Biochem. 34, 451 (1999)
- [37] W.J. Weber, J.C. Morris, J. Sanit. Eng. Div. AM Soc. Civ. Eng. 89, 31 (1963)
- [38] S.J. Allen, G. McKay, K.Y.H. Khader, Environ. Pollut. 56, 39 (1989)
- [39] Y.S. Ho, G. McKay, Process Biochem. 38, 1047 (2003)
- [40] G. McKay, M.S. Otterburn, J.A. Aga, Water Air Soil Pollut. 24, 307 (1985)
- [41] G. Bayramoglu, B. Altintas, M.Y. Arica, Chem. Eng. J. 152, 339 (2009)
- [42] N. Kannan, S. Murogavel, Global Nest J. 10, 395 (2008)
- [43] P. Vassileva, A. Detcheva, Int. J. Coal. Prep. Util. 31, 242 (2011)
- [44] E.S. Samra, Adsorpt. Sci. Technol. 18, 761 (2000)
- [45] M.M. Rao, G.P.C. Rao, K. Seshaiah, N.V. Choudary, M.C. Wang, Waste Manage. 28, 849 (2008)
- [46] M. Puanngam, F. Uno, J. Hazard. Mat. 154, 578 (2008)
- [47] P. Vassileva, D. Voikova, J. Hazard. Mat. 170, 948 (2009)
- [48] E.B. Reed, J. Maqbul, B. Tomas, Water Environ. Res. 68, 877 (1996)
- [49] M.J. Smith, Chemical Engineering Kinetics (McGraw-Hill Chemical Engineering Series, McGraw-Hill Companies, New York, 1981)